Metabolic Alterations Induced by Sucrose Intake and Alzheimer's Disease Promote Similar Brain Mitochondrial Abnormalities

Cristina Carvalho,[1,2] Susana Cardoso,[1,2] Sónia C. Correia,[1,2] Renato X. Santos,[1,2] Maria S. Santos,[1,2] Inês Baldeiras,[1,3] Catarina R. Oliveira,[1,4] and Paula I. Moreira[1,5]

Evidence shows that diabetes increases the risk of developing Alzheimer's disease (AD). Many efforts have been done to elucidate the mechanisms linking diabetes and AD. To demonstrate that mitochondria may represent a functional link between both pathologies, we compared the effects of AD and sucrose-induced metabolic alterations on mouse brain mitochondrial bioenergetics and oxidative status. For this purpose, brain mitochondria were isolated from wild-type (WT), triple transgenic AD (3xTg-AD), and WT mice fed 20% sucrose-sweetened water for 7 months. Polarography, spectrophotometry, fluorimetry, high-performance liquid chromatography, and electron microscopy were used to evaluate mitochondrial function, oxidative status, and ultrastructure. Western blotting was performed to determine the AD pathogenic protein levels. Sucrose intake caused metabolic alterations like those found in type 2 diabetes. Mitochondria from 3xTg-AD and sucrose-treated WT mice presented a similar impairment of the respiratory chain and phosphorylation system, decreased capacity to accumulate calcium, ultrastructural abnormalities, and oxidative imbalance. Interestingly, sucrose-treated WT mice presented a significant increase in amyloid β protein levels, a hallmark of AD. These results show that in mice, the metabolic alterations associated to diabetes contribute to the development of AD-like pathologic features. ***Diabetes*** **61:1234–1242, 2012**

Alzheimer's disease (AD) is a progressive neurodegenerative disorder that leads to dementia and affects approximately 10% of the population aged >65 years. AD is characterized by a severe neuronal loss and the presence of two brain lesions, senile plaques and neurofibrillary tangles, which are mainly constituted by amyloid β (Aβ) and hyperphosphorylated τ proteins, respectively (1).

Type 2 diabetes (T2D) is a well-known metabolic disorder that usually occurs in people aged >30 years and affects >7% of the global population. This disorder is characterized by a relative insulin deficiency, reduced insulin action, and insulin resistance of glucose transport, especially in skeletal muscle and adipose tissue. There is a cluster of risk factors for T2D and vascular disease that includes high blood glucose, obesity, increased blood triacylglycerols, and insulin resistance. All of these factors, individually and collectively, increase the risk of AD and vascular dementia. Epidemiological studies corroborate the idea that diabetes is a risk factor for vascular dementia and AD (2,3). AD and T2D share similar demographic profiles, risk factors, and perhaps more important, clinical and biochemical features (4).

Previous studies from our laboratory demonstrated that mitochondria isolated from the brains of T2D rats are more susceptible to Aβ protein exposure (5), suggesting that mitochondria are a functional link between diabetes and AD. Mitochondria play a critical role in the regulation of cell survival and death (6). These organelles are essential for the production of ATP through oxidative phosphorylation and regulation of intracellular calcium (Ca^{2+}) homeostasis. Thus, dysfunction of mitochondrial energy metabolism culminates in ATP production and Ca^{2+} buffering impairment and exacerbates the generation of reactive oxygen species (ROS). High levels of ROS cause, among other things, damage of cell membranes through lipid peroxidation and accelerate the high mutation rate of mitochondrial DNA. Accumulation of mitochondrial DNA mutations enhances oxidative damage, causes energy depletion, and increases ROS production in a vicious cycle (7). Moreover, the brain is especially prone to oxidative stress-induced damage due to its high levels of polyunsaturated fatty acids, high oxygen consumption, high content in transition metals, and poor antioxidant defenses.

The literature shows that mitochondrial dysfunction and oxidative stress are important in the early pathology of AD. Indeed, there are strong indications that oxidative stress occurs before the onset of symptoms in AD and that oxidative damage is found not only in the vulnerable regions of the brain affected in disease but also peripherally (8). Moreover, oxidative damage has been shown to occur before Aβ plaque formation (8), supporting a causative role of mitochondrial dysfunction and oxidative stress in AD.

Because we believe that brain mitochondria can be a functional bridge between diabetes (and prediabetic states) and AD, this study aimed to evaluate and compare the effect of sucrose-induced metabolic alterations and AD on mouse brain mitochondria. For this purpose, three groups of experimental animals were used: *1*) wild type (WT) control mice, *2*) sucrose-treated WT mice, and *3*) triple transgenic AD (3xTg-AD) mice. Sucrose solution was used because of compelling evidence showing that excessive consumption of sugars plays a key role in the epidemic of obesity and T2D (9).

From the [1]Center for Neuroscience and Cell Biology, University of Coimbra, Coimbra, Portugal; the [2]Department of Life Sciences–Faculty of Sciences and Technology, University of Coimbra, Coimbra, Portugal; the [3]Laboratory of Neurochemistry-Coimbra University Hospital and Neurology Department-Faculty of Medicine, University of Coimbra, Coimbra, Portugal; the [4]Institute of Biochemistry–Faculty of Medicine, University of Coimbra, Coimbra, Portugal; and the [5]Institute of Physiology–Faculty of Medicine, University of Coimbra, Coimbra, Portugal.

Corresponding author: Paula I. Moreira, venta@ci.uc.pt or pismoreira@gmail.com.

Received 24 August 2011 and accepted 26 January 2012.

DOI: 10.2337/db11-1186

This article contains Supplementary Data online at http://diabetes.diabetesjournals.org/lookup/suppl/doi:10.2337/db11-1186/-/DC1.

See accompanying commentary, p. 991.

Several parameters were evaluated: mitochondrial respiratory chain (respiratory states 2, 3, and 4, respiratory control ratio [RCR], and ADP/O index), phosphorylation system (mitochondrial transmembrane potential [$\Delta\Psi$m], ADP-induced depolarization, repolarization lag phase, and ATP-to-ADP ratio), Ca^{2+}-induced permeability transition pore (Ca^{2+} fluxes and mitochondrial ultrastructure), mitochondrial aconitase activity, hydrogen peroxide (H_2O_2) levels, and nonenzymatic (vitamin E, glutathione (GSH)-to-glutathione disulfide (GSSG) ratio) and enzymatic (glutathione reductase [GR], glutathione peroxidase [GPx]), and manganese superoxide dismutase [MnSOD]) antioxidant defenses. The levels of Aβ and phosphorylated τ (p-τ) proteins were also evaluated.

RESEARCH DESIGN AND METHODS

Animals. Male WT and 3xTg-AD mice (4 months old) were housed in our animal colony (Animal Facility, Faculty of Medicine/Center for Neuroscience and Cell Biology, University of Coimbra). WT mice were randomly divided into two groups: *1*) control group and *2*) sucrose-treated animals with free access to 20% sucrose solution during 7 months. Mice were maintained under controlled light (12-h day/night cycle) and humidity with free access (except in the fasting period) to water (WT and 3xTg-AD mice at basal conditions) or 20% sucrose solution (sucrose-treated WT) and powdered rodent chow (URF1; Charles River). Adhering to procedures approved by the Federation of Laboratory Animal Science Associations (FELASA), the animals (11 months old) were killed at the end of the treatment period by cervical displacement and decapitation.

Determination of biochemical parameters. Blood glucose, insulin, HBA_{1c}, triglycerides, and cholesterol levels were determined using standard procedures.

Isolation of brain mitochondria. Brain mitochondria were isolated from mice by the method of Moreira et al. (5), adding 0.02% digitonin to free mitochondria from the synaptosomal fraction.

Measurements of mitochondrial respiration. Oxygen consumption was registered polarographically with a Clark oxygen electrode (10) connected to a suitable recorder in a thermostated water-jacketed closed chamber with magnetic stirring. The reactions were carried out at 30°C in 1 mL of the standard medium (100 mmol/L sucrose, 100 mmol/L KCl, 2 mmol/L KH_2PO_4, 5 mmol/L Hepes, and 10 μmol/L EGTA, pH 7.4) with 0.5 mg protein. The respiratory state 2 of mitochondrial respiration was initiated with 5 mmol/L succinate (mitochondrial energization through complex II) in the presence of 2 μmol/L rotenone. RCR is the ratio between respiratory states 3 (consumption of oxygen in the presence of succinate and ADP) and 4 (consumption of oxygen after ADP has been consumed). The ADP/O index is expressed by the ratio between the amount of ADP added and the oxygen consumed during respiratory state 3.

Measurement of $\Delta\Psi_m$. $\Delta\Psi_m$ was monitored by evaluating the transmembrane distribution of the lipophilic cation tetraphenylphosphonium (TPP^+) with a TPP^+-selective electrode prepared according to Kamo et al. (11) using an Ag/AgCl-saturated electrode (Tacussel, model MI 402) as reference. TPP^+ uptake has been measured from the decreased TPP^+ concentration in the medium sensed by the electrode. The potential difference between the selective electrode and the reference electrode was measured with an electrometer and recorded continuously in a Linear 1200 recorder. Reactions were carried out in a chamber with magnetic stirring in 1 mL of the standard medium (100 mmol/L sucrose, 100 mmol/L KCl, 2 mmol/L KH_2PO_4, 5 mmol/L Hepes, and 10 μmol/L EGTA; pH 7.4) containing 3 μmol/L TPP^+. Mitochondria (0.5 mg/mL) were energized with 5 mmol/L succinate in the presence of 2 μmol/L rotenone. After a steady-state distribution of TPP^+ had been reached (~1 min of recording), $\Delta\Psi_m$ fluctuations were recorded.

Determination of adenine nucleotide levels. Adenine nucleotides were evaluated by separation in a reverse-phase high-performance liquid chromatography.

Measurement of Ca^{2+} fluxes. Mitochondrial Ca^{2+} fluxes were measured by monitoring the changes in Ca^{2+} concentration in the reaction medium using a Ca^{2+}-selective electrode (12).

Electron microscopy. Mitochondrial fractions were fixed for electron microscopy by the addition of 3% glutaraldehyde in 0.1 mol/L phosphate buffer (pH 7.3) and incubated for 2 h at 4°C. After preincubation in 1% agar, samples were dehydrated in grade ethanol and embedded in Spurr. The ultrathin sections were obtained in an LKB ultramycrotome Ultrotome III, stained with methanolic uranyl acetate, followed by lead citrate, and examined with a Jeol Jem-100SV electron microscope operated at 80 kV.

Measurement of aconitase activity. Aconitase activity was determined according to Krebs and Holzach (13).

Measurement of H_2O_2 levels. H_2O_2 levels were measured fluorimetrically using a modification of the method described by Barja (14).

Measurement of GSH and GSSG levels. GSH and GSSG levels were determined with fluorescence detection after reaction of the supernatants from deproteinized mitochondria containing H_3PO_4/NaH_2PO_4-EDTA or H_3PO_4/NaOH, respectively, with *o*-phthalaldehyde (pH 8.0) according to Hissin and Hilf (15).

Measurement of vitamin E content. Extraction and separation of vitamin E (α-tocopherol) from brain mitochondria were performed by following a previously described method by Vatassery and Younoszai (16).

Measurement of GPx, GR, and SOD activities. The activities of GPx (17), GR (18), and SOD (19) were determined spectrophotometrically, as previously described.

Evaluation of Aβ and p-τ proteins levels. Brains were homogenized in buffer containing 50 mmol/L Tris-HCl, 150 mmol/L NaCl, 1% NP-40, 1% deoxycorticosterone, and 0.1% SDS (pH 7.4), protease inhibitors (commercial protease inhibitor cocktail from Roche), phosphatase inhibitors (commercial phosphatase inhibitor cocktail from Roche), 0.1 mol/L phenylmethylsulfonyl fluoride (Sigma), 0.2 mol/L dithiothreitol (Sigma), frozen three times in liquid nitrogen, and centrifuged at 13,200*g* for 10 min. The blots were subsequently incubated with the respective primary antibodies overnight at 4°C with gentle agitation (1:1,000 mouse monoclonal human β amyloid [clone 6E10] from Signet Laboratories; 1:1000 mouse monoclonal paired helical filament-τ monoclonal antibody [clone AT8] from Thermo Fisher Scientific; or 1:10,000 monoclonal anti–α-tubulin antibody from Sigma). Fluorescence signals were detected using a Bio-Rad Versa-Doc Imager, and band densities were determined using Quantity One Software.

Statistical analysis. Results are presented as mean ± SEM of the indicated number of experiments. Statistical significance was determined using the paired student *t* test and Kruskal-Wallis test for multiple comparisons, followed by the post hoc Dunn test.

RESULTS

Characterization of experimental animals. Compared with WT mice, 3xTg-AD animals presented a significant decrease in body and brain weight, and consequently, a decrease in brain weight-to-body weight ratio (Table 1). These

TABLE 1
Characterization of animals

	WT control	WT sucrose	3xTg-AD
Body weight (g)	35.20 ± 1.09	42.86 ± 1.27***	31.14 ± 0.7485**
Brain weight (g)	1.06 ± 0.07	0.75 ± 0.08*	0.76 ± 0.09*
Brain weight-to-body weight ratio	0.03 ± 0.002	0.02 ± 0.002**	0.02 ± 0.002**
Postprandial glycemia (mg/dL)	100.70 ± 2.19	116.60 ± 3.72*	121.30 ± 8.53*
Occasional glycemia (mg/dL)	122.40 ± 7.90	144.00 ± 5.58*	117.10 ± 7.86
Insulin levels (μg/L)	0.44 ± 0.08	0.68 ± 0.23	0.36 ± 0.02
HbA_{1c} (%)	3.36 ± 0.07	3.77 ± 0.08**	3.99 ± 0.11***
Triglyceride levels (mg/dL)	159.80 ± 19.16	277.40 ± 30.60**	168.20 ± 17.80
Cholesterol levels (mg/dL)	161.30 ± 2.81	160.10 ± 1.91	160.60 ± 2.48

Data represent mean ± SEM from 10 to 12 animals. *$P < 0.05$; **$P < 0.01$; ***$P < 0.001$ compared with WT control animals.

animals also presented an increase in HbA_{1c} and postprandial glucose levels (Table 1). In WT mice, sucrose intake promoted an increase in body weight, a decrease in brain weight, and consequently, a decrease in brain weight-to-body weight ratio compared with WT mice under basal conditions. In addition, sucrose intake promoted an increase in HbA_{1c}, blood glucose, and insulin and triglycerides levels (Table 1) and a decrease in glucose tolerance (Supplementary Fig. 1) compared with the respective control mice. No alterations in cholesterol levels were observed (Table 1).

AD and sucrose-induced metabolic alterations impair mitochondrial respiratory chain and oxidative phosphorylation system. Sucrose-treated WT animals present an increase in respiratory states 2 (~35 and ~41%, respectively) and 4 (~46 and ~54%, respectively) and a decrease in respiratory state 3 (~33 and ~31%, respectively) and RCR (~15 and ~17%, respectively; Fig. 1). No significant changes were observed in the ADP/O index (Fig. 1). The mitochondrial transmembrane potential ($\Delta\Psi_m$) is fundamental for the phenomenon of oxidative phosphorylation, which results in the conversion of ADP to ATP via ATP synthase. Compared with mitochondria isolated from WT control mice, mitochondria from 3xTg-AD and sucrose-treated WT mice presented a significant decrease in $\Delta\Psi_m$ (~9 and ~7%, respectively), ADP-induced depolarization (~23% in both groups) and ATP-to-ADP ratio (~48 and ~42%, respectively), and a significant increase in the repolarization lag phase, the time needed to phosphorylate exogenous ADP (~37 and ~40%, respectively; Table 2).

AD and sucrose-induced metabolic alterations potentiate the opening of the mitochondrial permeability transition pore induced by Ca^{2+}. The mitochondrial permeability transition pore (PTP) is characterized by an increase in mitochondrial membrane permeability that leads to the loss of $\Delta\Psi_m$, alteration in Ca^{2+} fluxes, mitochondrial swelling, and rupture of mitochondrial membranes and cristae (5,6). In the presence of 80 nmol Ca^{2+}, mitochondria isolated from 3xTg-AD (Fig. 2*A*, *trace 6*) and sucrose-treated WT (Fig. 2*A*, *trace 5*) animals accumulated and retained less Ca^{2+} compared with WT control mitochondria (Fig. 2*A*, *trace 4*). The pair oligomycin/ADP (Fig. 2*A*, *traces 1*, *2*, and *3*), which is more effective than cyclosporine A in preventing PTP opening in brain mitochondria (5), significantly increased the capacity of mitochondria to accumulate and retain Ca^{2+}. Concerning ultrastructure, mitochondria from sucrose-treated animals (Fig. 2*B*, 2) and 3xTg-AD (Fig. 2*B*, 3) present a high percentage of damaged mitochondria, characterized by swollen mitochondria with disrupted mitochondrial membranes and cristae compared with WT control mitochondria (Fig. 2*B*, 1).

AD and sucrose-induced metabolic alterations promote oxidative stress and damage. Mitochondrial aconitase activity is a sensitive redox sensor of reactive oxygen and nitrogen species in cells. Brain mitochondria isolated from 3xTg-AD mice presented a significant decrease (~54%) in aconitase activity compared with WT control mitochondria (Fig. 3*A*). Interestingly, sucrose-treated WT animals showed a similar decrease (~51%) in aconitase activity compared with 3xTg-AD mice. Accordingly, a significant increase in H_2O_2 levels was observed in mitochondria from both 3xTg-AD (~25%) and sucrose-treated WT (~18%) mice (Fig. 3*B*).

AD and sucrose-induced metabolic alterations impair antioxidant defenses. Glutathione and vitamin E are important intracellular antioxidants, acting as free radical

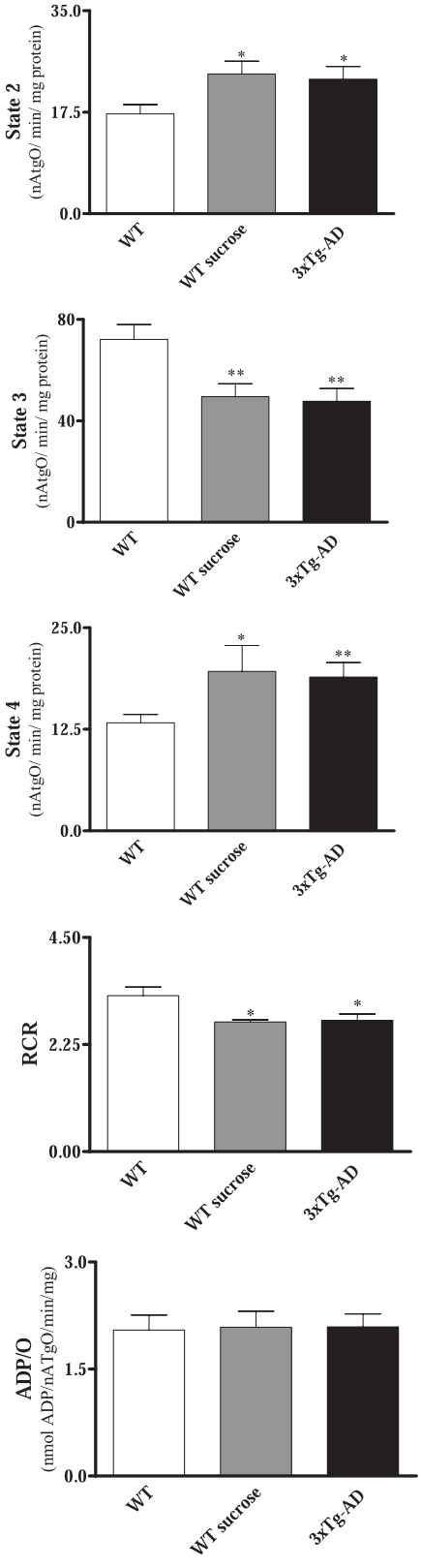

FIG. 1. Effects of AD and sucrose-induced metabolic alterations on mitochondrial respiration. The respiratory states 2, 3, and 4 and RCR and ADP/O index were evaluated in freshly isolated brain mitochondrial fractions (0.5 mg) in 1 mL of the reaction medium energized with 5 mmol/L succinate in the presence of 2 μmol/L rotenone. Data shown represent means ± SEM of five to six independent experiments. nAtgO/min/mg, nAtom-gram oxygen/min/mg. *$P < 0.05$; **$P < 0.01$.

TABLE 2
Effects of AD and sucrose intake on the mitochondrial oxidative phosphorylation system

	WT control	WT sucrose	3xTg-AD
ΔΨm (–mV)	219.90 ± 4.11	202.90 ± 2.95**	199.10 ± 1.69***
ADP-induced depolarization (–mV)	30.60 ± 1.99	23.23 ± 2.19*	23.56 ± 2.51*
Repolarization lag phase (min)	1.64 ± 0.19	2.30 ± 0.23*	2.24 ± 0.17*
ATP-to-ADP ratio	8.59 ± 1.02	4.95 ± 1.13**	4.45 ± 1.33*

The oxidative phosphorylation parameters were evaluated in freshly isolated brain mitochondrial fractions (0.5 mg) in 1 mL of the reaction medium supplemented with 3 μmol/L TPP^+ and energized with 5 mmol/L succinate in the presence of 2 μmol/L rotenone. Adenine nucleotide levels were determined by high-performance liquid chromatography, as described in RESEARCH DESIGN AND METHODS. Data shown represent mean ± SEM from five to six independent experiments. *$P < 0.05$; **$P < 0.01$; ***$P < 0.001$ compared with WT control animals.

scavengers and, consequently, protecting cells against oxidative damage. Brain mitochondria isolated from 3xTg-AD and sucrose-treated WT animals present a significant decrease in the GSH-to-GSSG ratio (~60 and 64%, respectively; Fig. 4*A*) and vitamin E levels (~60 and 64%, respectively; Fig. 4*B*) compared with WT mitochondria.

GPx and GR are two antioxidant enzymes involved in the detoxification of ROS. GPx catalyzes the reduction of H_2O_2 and various hydroperoxides to water. In addition, GR is responsible for regenerating GSH from GSSG using NADPH as an H^+ donor. Compared with WT mice, mitochondria isolated from 3xTg-AD and sucrose-treated WT animals present a significant increase in the activity of GPx (~38 and ~48%, respectively) and a decrease in GR activity (~70 and ~62%, respectively; Fig. 5*A* and *B*). MnSOD activity is significantly increased in 3xTg-AD (~375%) and sucrose-treated WT animals (~318%) compared with WT control animals (Fig. 5*C*).

Sucrose-induced metabolic alterations increase Aβ protein levels. Not surprisingly, 3xTg-AD mice present high levels of Ab protein. However, WT under sucrose intake also presented a significant increase in the levels of Aβ protein, particularly in the cortex. An increase in p-τ protein levels was also observed, although not statistically significant (Fig. 6).

DISCUSSION

This study shows that metabolic alterations associated with sucrose intake promoted an impairment of the brain mitochondrial respiratory chain, oxidative phosphorylation system, and Ca^{2+} homeostasis, as well as an oxidative imbalance similar to those observed in the 3xTg-AD mouse model. Furthermore, a significant increase in the levels of Aβ protein, a hallmark of AD, was observed in brain tissue of sucrose-treated mice.

Sucrose intake in WT mice impaired glucose tolerance (Supplementary Fig. 1) and increased blood glucose, HbA_{1c}, insulin, and triglycerides levels (Table 1). A significant increase in body weight and a decrease in brain weight and in the brain weight-to-body weight ratio (Table 1) were also observed in sucrose-treated WT and 3xTg-AD mice. Previous studies showed that diabetes is associated to a gain in body weight and a decrease in overall brain weight (20). The alterations induced by sucrose intake indicate that these animals are in a (pre)diabetic state (21). Several studies showed that phenotypes associated with obesity and/or alterations on insulin homeostasis are at increased risk for developing cognitive decline and dementia, namely vascular dementia and AD (22). A recent study also showed that multiple vascular risk factors are associated with a greater rate of decline in cognition, function, and regional cerebral blood flow in AD patients, which highlights the contribution of vascular risk factors on the progression of AD (23). Furthermore, there is published literature showing that diabetes influences the survival of AD patients (24).

Interestingly, an increase in HbA_{1c} levels in 3xTg-AD mice under basal conditions was also observed, which may represent a consequence of the altered glucose metabolism occurring in AD. This idea is reinforced by the observation that these AD mice presented an increase in postprandial blood glucose levels (Table 1). HbA_{1c} is an early glycation product and one precursor of advanced glycation end products (AGEs) (25). Previous studies demonstrated that the interaction of AGEs with their receptor, named RAGE, elicits the formation of ROS that are also believed to be an early event in AD pathology (26).

3xTg-AD animals under basal conditions also presented a decrease in body and brain weight and, consequently, in brain weight-to-body weight ratio (Table 1), characteristics also observed in AD patients (27,28). Indeed, weight loss is a frequent complication of AD and occurs in 40% of patients at all disease stages (27,28).

To show that brain mitochondria may represent a functional link between diabetes (and prediabetic states) and AD, we evaluated and compared the effect of sucrose-induced metabolic alterations and AD in mitochondrial bioenergetics and oxidative status. Previous studies from our laboratory showed that the synthetic Aβ25–35 and Aβ1−40 peptides impair the respiratory chain, uncouple the oxidative phosphorylation system, and decrease ATP levels of isolated brain mitochondria (5). More recently, Dragicevic et al. (29) evaluated the function of mitochondria isolated from several brain regions obtained from 12-month APPsw and APP+PS1 mouse models of AD. The authors observed an impairment of the respiratory chain and a decrease in ΔΨm in both animal models, these defects being more pronounced in hippocampal and cortical mitochondria (29). Accordingly, we observed that mitochondria from 3xTg-AD animals present an impairment of the respiratory chain (Fig. 1) and phosphorylation system, culminating in lower production of ATP (Table 2). This ATP deficit was also observed in mitochondria isolated from AD platelets (30). The low levels of cellular ATP may result in the loss of synapses and synaptic function leading to cognitive decline (31). Interestingly, mitochondria isolated from sucrose-treated WT animals present a similar pattern of respiratory chain and oxidative phosphorylation system impairment (Fig. 1, Table 2), supporting the idea that mitochondrial dysfunction is a common denominator between diabetes (and prediabetic states) and AD.

The PTP is a nonselective, high-conductance channel that spans the inner and outer mitochondrial membranes (32).

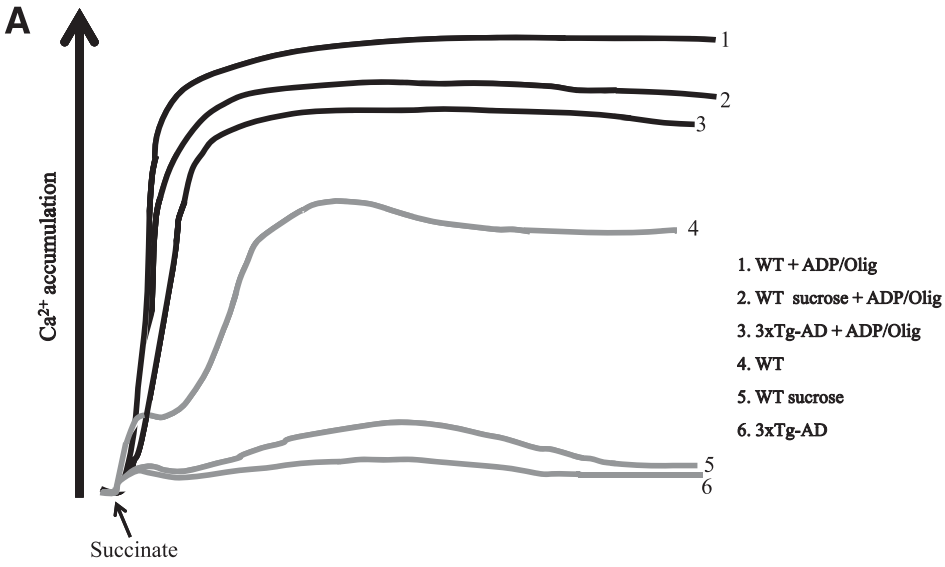

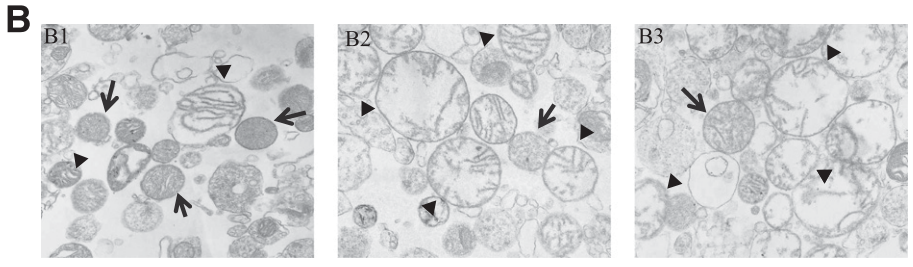

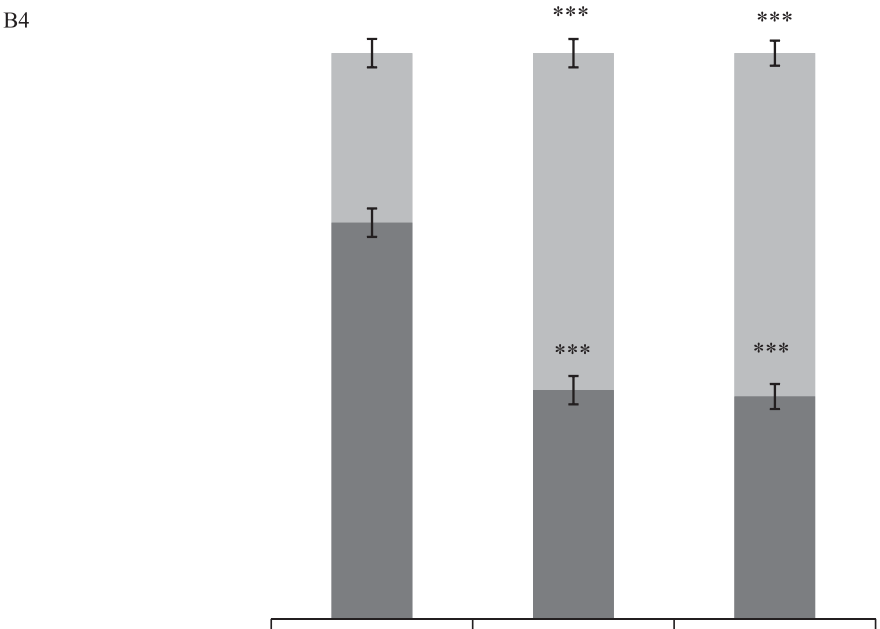

	WT	WT sucrose	3xTg-AD
% Damaged mitochondria	29.96	59.56	60.68
% Normal mitochondria	70.04	40.44	39.32

FIG. 2. Effects of AD and sucrose-induced metabolic alterations on mitochondrial Ca^{2+} fluxes and ultrastructure. *A*: Freshly isolated brain mitochondria (0.5 mg) in 1 mL of the reaction medium were energized with 5 mmol/L succinate. Ca^{2+} (80 nmol/mg protein) was added 1 min before mitochondria energization. Oligomycin (0.2 μg/mL) plus ADP (100 μmol/L) were added 2 min before Ca^{2+} addition. The traces are typical of five to six independent experiments. Trace 1: WT control mitochondria in the presence of oligomycin plus ADP; trace 2: WT sucrose-treated mitochondria in the presence of oligomycin plus ADP; trace 3: 3xTg-AD mitochondria in the presence of oligomycin plus ADP; trace 4: WT control; trace 5: WT sucrose-treated mitochondria; trace 6: 3xTg-AD mitochondria. *B*: After calcium experiments, mitochondria were fixed for electron microscopy. Images represent WT control mitochondria (*B1*); WT sucrose-treated mitochondria (*B2*); 3xTg-AD mitochondria (*B3*) in the presence of Ca^{2+} (80 nmol/mg protein), and graphic representation of normal and damaged mitochondria (*B4*). *Arrows*, Normal mitochondria; *arrowheads*, damaged mitochondria. ***$P < 0.001$ compared with WT control mitochondria.

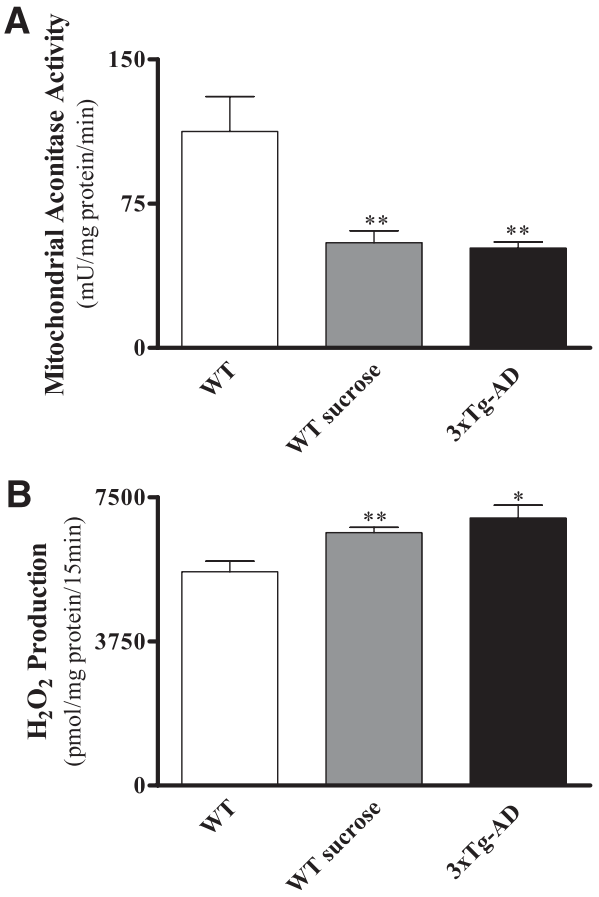

FIG. 3. Effects of AD and sucrose-induced metabolic alterations on mitochondrial oxidative stress. *A*: Aconitase activity. *B*: H_2O_2 levels. Data shown represent mean ± SEM from five to six independent experiments. **P* < 0.05; ***P* < 0.01 compared with WT control animals.

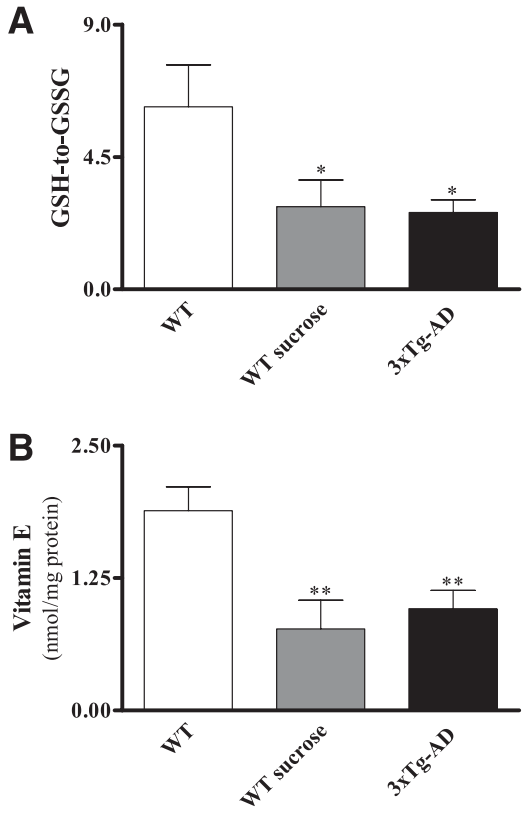

FIG. 4. Effects of AD and sucrose-induced metabolic alterations on nonenzymatic antioxidant defenses. GSH-to-GSSG ratio (*A*) and vitamin E levels (*B*). Data shown represent means ± SEM from five to six independent experiments. **P* < 0.05; ***P* < 0.01 compared with WT control animals.

Mitochondria can tolerate a certain amount of Ca^{2+}, but ultimately, their capacity to adapt to Ca^{2+} loads is overwhelmed, and mitochondria depolarize completely due to a profound change in the inner membrane permeability, reflecting PTP induction (33). Although Ca^{2+} is considered to be the most important inducer, matrix pH, $\Delta\Psi m$, Mg^{2+}, Pi, cyclophilin D, oxidative stress, and adenine nucleotides are also effective regulators (34). In addition, PTP plays an important role in the apoptotic process by releasing several apoptogenic factors such as cytochrome c (32). In the current study, mitochondria from 3xTg-AD and sucrose-treated WT mice presented a decreased capacity to accumulate and retain Ca^{2+} (Fig. 2*A*). These results are in accordance with previous studies from our laboratory showing that isolated brain mitochondria exposed to synthetic Aβ peptides present a lower capacity to accumulate and retain Ca^{2+} (5). Du et al. (35) reported that synaptic mitochondria from mutant APP mice show an age-dependent accumulation of Aβ and mitochondrial alterations characterized by a decrease in cytochrome oxidase activity and respiration and an increase in oxidative stress and mitochondrial permeability transition. Furthermore, it was shown that the overactivation of *N*-methyl-D-aspartate (NMDA) and α-amino-3-hydroxy-5-methyl-4-isoxazolepropionic acid (AMPA) receptors, mitochondrial Ca^{2+} overload, and mitochondrial damage underlie the neurotoxicity induced by Aβ oligomers (36). We also showed that brain mitochondria isolated from diabetic rats exposed to Aβ peptides are more susceptible to Ca^{2+}-induced PTP opening compared with mitochondria from control animals (5). The capacity of mitochondria to accumulate and retain Ca^{2+} was significantly increased by the presence of ADP plus oligomycin (Fig. 2*A*). Although cyclosporine A is considered the specific inhibitor of PTP, previous studies demonstrated that the pair ADP plus oligomycin is more effective in preventing PTP in brain mitochondria (5). In accordance with Ca^{2+} fluxes data, our electron microscopy analyses revealed that 3xTg-AD and sucrose-treated WT animals have a high percentage of damaged mitochondria characterized by mitochondrial swelling and rupture of mitochondrial membranes and cristae (Fig. 2*B*).

Because mitochondria are major intracellular sources of ROS, we also evaluated the oxidative status of our brain mitochondrial preparations. We observed an increased production of H_2O_2 in 3xTg-AD and sucrose-treated WT mice (Fig. 3*B*), which is positively correlated with the increased susceptibility to PTP opening (Fig. 2). Indeed, a rise in the production of endogenous mitochondrial ROS, including H_2O_2, was previously reported to facilitate PTP opening (37). Manczak et al. (38) also observed a significant increase in the levels of H_2O_2 in Tg2576 mice compared with age-matched WT littermates before the appearance of Aβ plaques. The increase in mitochondrial ROS production is positively correlated with the decrease in the activity of mitochondrial aconitase in 3xTg-AD and sucrose-treated WT animals (Fig. 3*A*). A major role has been proposed for the reaction between mitochondrial aconitase and superoxide in mitochondrial oxidative damage (39). Aconitase

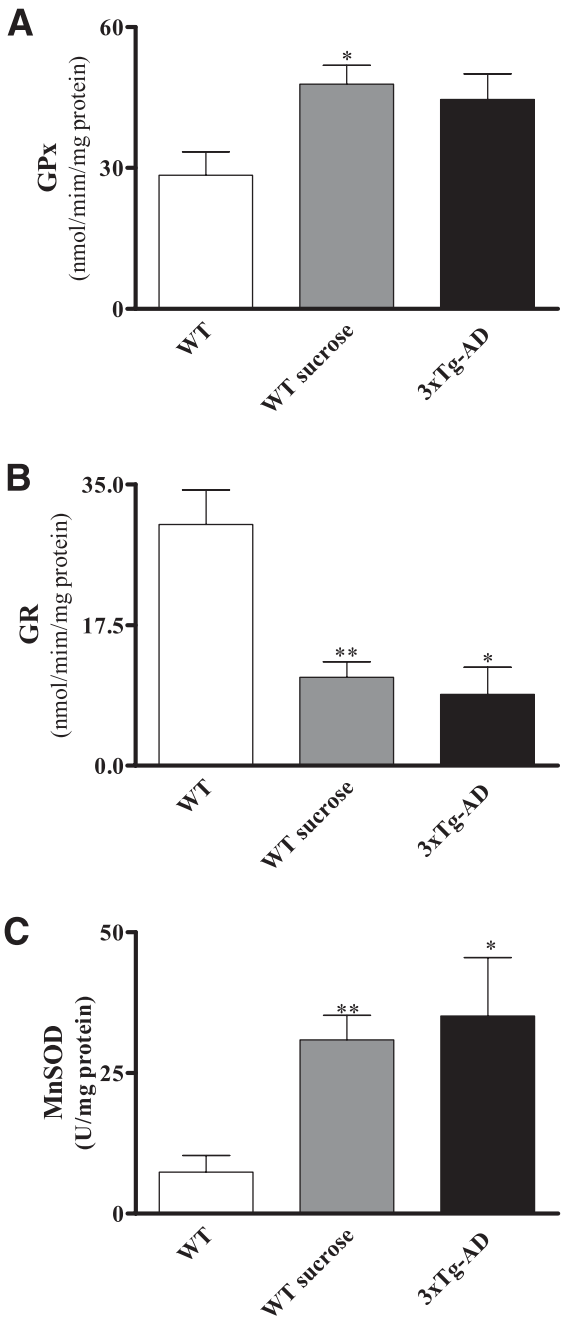

FIG. 5. Effects of AD and sucrose-induced metabolic alterations on enzymatic antioxidant defenses. *A*: GPx activity. *B*: GR activity. *C*: MnSOD activity. Data shown represent means ± SEM from five to six independent experiments. *$P < 0.05$; **$P < 0.01$ compared with WT control animals.

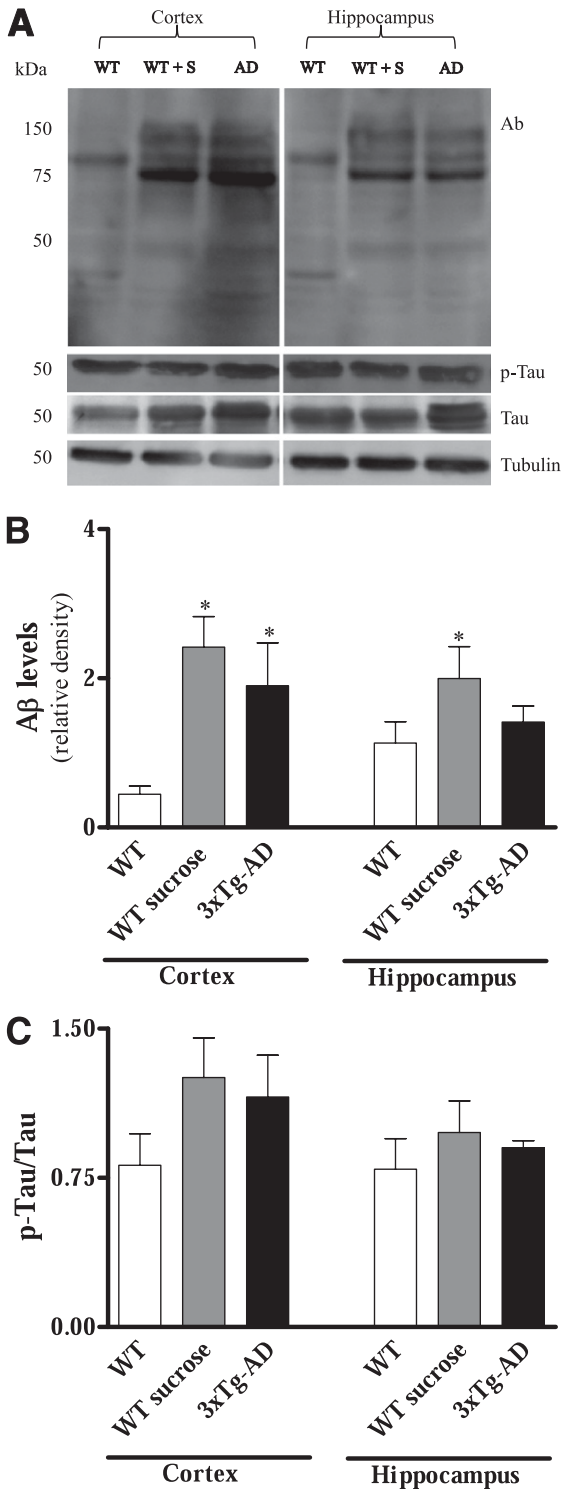

FIG. 6. Effects of AD and sucrose-induced metabolic alterations on Aβ and p-τ proteins levels. Western blotting detection (*A*) and density of bands (*B*) corresponding to Aβ and total and p-τ proteins. WT + *S*, WT sucrose-treated animals; AD, 3xTg-AD control animals.

has an iron-sulfur cluster in its active center that is highly sensitive to superoxide and other reactive species, which inactivates the enzyme (40). A decrease in aconitase activity was also demonstrated in several experimental models of neurodegenerative diseases (41).

Because oxidative stress is caused by an imbalance between ROS production and the ability of the biologic system to readily detoxify the reactive intermediates or easily repair the resulting damage via antioxidant defenses (26), we also evaluated several enzymatic and nonenzymatic antioxidant defenses. One key cellular antioxidant is GSH, a potent free radical scavenger and the cosubstrate of the antioxidant enzyme GPx. Intracellular GSH is converted into GSSG by GPx, which catalyzes the reduction of H_2O_2 and various hydroperoxides (42). GR is also responsible for regenerating GSH from GSSG using NADPH as an H^+ donor (43). Several studies have reported alterations in glutathione levels in AD and diabetes (44,45). Accordingly, we observed that brain mitochondria from 3xTg-AD control and

sucrose-treated WT animals present a significant decrease in the GSH-to-GSSG ratio (Fig. 4*A*). Also, a decrease in GR activity and an increase in GPx in these two groups of experimental animals (Fig. 5*A* and *B*) were observed, justifying the decrease in GSH levels (Fig. 4*A*). We have previously shown that brain tissue from 3- to 5-month-old female 3xTg-AD mice present lower levels of GSH and vitamin E and an increased activity of SOD and GPx (46). Accordingly, we also observed a significant decrease in vitamin E levels in 3xTg-AD and sucrose-treated WT animals (Fig. 4*B*). A decrease in vitamin E levels was also observed in the plasma of diabetic (47) and AD (48) patients. An increase in MnSOD activity in 3xTg-AD and WT sucrose-treated mice (Fig. 5*C*) was also observed, which is consistent with the increase in H_2O_2 levels observed in these animals (Fig. 3*B*). SOD catalyzes the conversion of superoxide to H_2O_2 and its activity is undoubtedly important to the regulation of oxidative status. These results are in accordance with previous results obtained in AD fibroblasts cell lines, where MnSOD activity was significantly elevated by 30% compared with normal euploid cell lines (49).

Another interesting finding is that metabolic alterations induced by sucrose intake increase the levels of Aβ and (slightly) p-τ proteins (Fig. 6), hallmarks of AD, which supports the idea that (pre)diabetes is a risk factor for AD. Accordingly, it was previously shown that T2D BBZDR/Wor rats and type 1 diabetic BB/Wor rats present brain accumulation of Aβ and p-τ proteins, this accumulation being more pronounced in T2D rats (50).

In summary, our results show that in mouse models, the metabolic alterations associated to diabetic or prediabetic conditions induce mitochondrial abnormalities, an oxidative imbalance, and an increase in Aβ protein levels similar to those found in AD brains.

ACKNOWLEDGMENTS

The authors' work is supported by the Fundação para a Ciência e a Tecnologia (FCT) and Fundo Europeu de Desenvolvimento Regional (PTDC/SAU-NEU/103325/2008) and Quadro de Referência Estratégico Nacional (QREN DO-IT).

C.C. has a PhD fellowship from FCT (SFRH/BD/43965/2008).

No potential conflicts of interest relevant to this article were reported.

C.C. researched data, contributed to discussion, and wrote the manuscript. S.C., S.C.C, R.X.S., and I.B. researched data. M.S.S., C.R.O., and P.I.M. contributed to discussion and reviewed and edited the manuscript. P.I.M. is the guarantor of this work and, as such, had full access to all of the data in the study and takes responsibility for the integrity of the data and the accuracy of the data analysis.

The authors are sincerely grateful to Dr. Frank LaFerla, from the University of California, for the gift of 3xTg-AD mice and the corresponding WT mice.

REFERENCES

1. Khachaturian ZS. Diagnosis of Alzheimer's disease. Arch Neurol 1985;42:1097–1105
2. Kalaria RN, Maestre GE, Arizaga R, et al.; World Federation of Neurology Dementia Research Group. Alzheimer's disease and vascular dementia in developing countries: prevalence, management, and risk factors. Lancet Neurol 2008;7:812–826
3. Roriz-Filho JS, Sá-Roriz TM, Rosset I, et al. (Pre)diabetes, brain aging, and cognition. Biochim Biophys Acta 2009;1792:432–443
4. Selkoe DJ. Alzheimer's disease: genotypes, phenotypes, and treatments. Science 1997;275:630–631
5. Moreira PI, Santos MS, Moreno AM, Seiça R, Oliveira CR. Increased vulnerability of brain mitochondria in diabetic (Goto-Kakizaki) rats with aging and amyloid-beta exposure. Diabetes 2003;52:1449–1456
6. Moreira PI, Carvalho C, Zhu X, Smith MA, Perry G. Mitochondrial dysfunction is a trigger of Alzheimer's disease pathophysiology. Biochim Biophys Acta 2010;1802:2–10
7. Correia SC, Carvalho C, Cardoso S, et al. Mitochondrial preconditioning: a potential neuroprotective strategy. Front Aging Neurosci 2010;2:138–150
8. Nunomura A, Perry G, Aliev G, et al. Oxidative damage is the earliest event in Alzheimer disease. J Neuropathol Exp Neurol 2001;60:759–767
9. Cao D, Lu H, Lewis TL, Li L. Intake of sucrose-sweetened water induces insulin resistance and exacerbates memory deficits and amyloidosis in a transgenic mouse model of Alzheimer disease. J Biol Chem 2007;282:36275–36282
10. Estabrook RE. Mitochondrial respiratory control and the polarographic measurement of ADP/O ratios. Methods Enzymol 1967;10:41–47
11. Kamo N, Muratsugu M, Hongoh R, Kobatake Y. Membrane potential of mitochondria measured with an electrode sensitive to tetraphenyl phosphonium and relationship between proton electrochemical potential and phosphorylation potential in steady state. J Membr Biol 1979;49:105–121
12. Moreno AJM, Madeira VMC. Mitochondrial bioenergetics as affected by DDT. Biochim Biophys Acta 1991;1060:166–174
13. Krebs HA, Holzach O. The conversion of citrate into cis-aconitate and isocitrate in the presence of aconitase. Biochem J 1952;52:527–528
14. Barja G. Mitochondrial oxygen radical generation and leak: sites of production in states 4 and 3, organ specificity, and relation to aging and longevity. J Bioenerg Biomembr 1999;31:347–366
15. Hissin PJ, Hilf RA. A fluorometric method for determination of oxidized and reduced glutathione in tissues. Anal Biochem 1976;74:214–226
16. Vatassery GT, Younoszai R. Alpha tocopherol levels in various regions of the central nervous systems of the rat and guinea pig. Lipids 1978;13:828–831
17. Flohé L, Günzler WA. Assays of glutathione peroxidase. Methods Enzymol 1984;105:114–121
18. Carlberg I, Mannervik B. Glutathione reductase. Methods Enzymol 1985;113:484–490
19. Flohé L, Otting F. Superoxide dismutase assays. Methods Enzymol 1984;105:93–104
20. Wuarin L, Namdev R, Burns JG, Fei ZJ, Ishii DN. Brain insulin-like growth factor-II mRNA content is reduced in insulin-dependent and non-insulin-dependent diabetes mellitus. J Neurochem 1996;67:742–751
21. Hsueh WA, Orloski L, Wyne K. Prediabetes: the importance of early identification and intervention. Postgrad Med 2010;122:129–143
22. Luchsinger JA, Tang MX, Shea S, Mayeux R. Hyperinsulinemia and risk of Alzheimer disease. Neurology 2004;63:1187–1192
23. Kume K, Hanyu H, Sato T, et al. Vascular risk factors are associated with faster decline of Alzheimer disease: a longitudinal SPECT study. J Neurol 2011;258:1295–1303
24. Magierski R, Kłoszewska I, Sobów TM. The influence of vascular risk factors on the survival rate of patients with dementia with Lewy bodies and Alzheimer disease. Neurol Neurochir Pol 2010;44:139–147
25. Makita Z, Vlassara H, Rayfield E, et al. Hemoglobin-AGE: a circulating marker of advanced glycosylation. Science 1992;258:651–653
26. Carvalho C, Correia SC, Santos RX, et al. Role of mitochondrial-mediated signaling pathways in Alzheimer disease and hypoxia. J Bioenerg Biomembr 2009;41:433–440
27. Guyonnet S, Nourhashemi F, Andrieu S. A prospective study in the nutritional status of Alzheimer's patients. Arch Gerontol Geriatr 1998;6:255–262
28. Power DA, Noel J, Collins R, O'Neill D. Circulating leptin levels and weight loss in Alzheimer's disease patients. Dement Geriatr Cogn Disord 2001;12:167–170
29. Dragicevic N, Mamcarz M, Zhu Y, et al. Mitochondrial amyloid-beta levels are associated with the extent of mitochondrial dysfunction in different brain regions and the degree of cognitive impairment in Alzheimer's transgenic mice. J Alzheimers Dis 2010;20(Suppl. 2):S535–S550
30. Cardoso SM, Proença MT, Santos S, Santana I, Oliveira CR. Cytochrome c oxidase is decreased in Alzheimer's disease platelets. Neurobiol Aging 2004;25:105–110
31. Butterfield DA, Perluigi M, Sultana R. Oxidative stress in Alzheimer's disease brain: new insights from redox proteomics. Eur J Pharmacol 2006;545:39–50
32. Bernardi P, Broekemeier KM, Pfeiffer DR. Recent progress on regulation of the mitochondrial permeability transition pore; a cyclosporin-sensitive pore in the inner mitochondrial membrane. J Bioenerg Biomembr 1994;26:509–517
33. Carvalho C, Correia S, Santos MS, Seiça R, Oliveira CR, Moreira PI. Metformin promotes isolated rat liver mitochondria impairment. Mol Cell Biochem 2008;308:75–83

34. Fontaine E, Eriksson O, Ichas F, Bernardi P. Regulation of the permeability transition pore in skeletal muscle mitochondria. Modulation By electron flow through the respiratory chain complex i. J Biol Chem 1998;273:12662–12668
35. Du H, Guo L, Yan S, Sosunov AA, McKhann GM, Yan SS. Early deficits in synaptic mitochondria in an Alzheimer's disease mouse model. Proc Natl Acad Sci USA 2010;107:18670–18675
36. Alberdi E, Sánchez-Gómez MV, Cavaliere F, et al. Amyloid beta oligomers induce Ca2+ dysregulation and neuronal death through activation of ionotropic glutamate receptors. Cell Calcium 2010;47:264–272
37. Kowaltowski AJ, Castilho RF, Vercesi AE. Mitochondrial permeability transition and oxidative stress. FEBS Lett 2001;495:12–15
38. Manczak M, Anekonda TS, Henson E, Park BS, Quinn J, Reddy PH. Mitochondria are a direct site of A beta accumulation in Alzheimer's disease neurons: implications for free radical generation and oxidative damage in disease progression. Hum Mol Genet 2006;15:1437–1449
39. Gardner PR, Raineri I, Epstein LB, White CW. Superoxide radical and iron modulate aconitase activity in mammalian cells. J Biol Chem 1995;270:13399–13405
40. Vasquez-Vivar J, Kalyanaraman B, Kennedy MC. Mitochondrial aconitase is a source of hydroxyl radical. An electron spin resonance investigation. J Biol Chem 2000;275:14064–14069
41. Patel M, Day BJ, Crapo JD, Fridovich I, McNamara JO. Requirement for superoxide in excitotoxic cell death. Neuron 1996;16:345–355
42. Durmaz A, Dikmen N. Homocysteine effects on cellular glutathione peroxidase (GPx-1) activity under in vitro conditions. J Enzyme Inhib Med Chem 2007;22:733–738
43. Rauscher FM, Sanders RA, Watkins JB 3rd. Effects of isoeugenol on oxidative stress pathways in normal and streptozotocin-induced diabetic rats. J Biochem Mol Toxicol 2001;15:159–164
44. Liu H, Wang H, Shenvi S, Hagen TM, Liu RM. Glutathione metabolism during aging and in Alzheimer disease. Ann N Y Acad Sci 2004;1019:346–349
45. Mastrocola R, Restivo F, Vercellinatto I, et al. Oxidative and nitrosative stress in brain mitochondria of diabetic rats. J Endocrinol 2005;187:37–44
46. Resende R, Moreira PI, Proença T, et al. Brain oxidative stress in a triple-transgenic mouse model of Alzheimer disease. Free Radic Biol Med 2008;44:2051–2057
47. Peerapatdit T, Patchanans N, Likidlilid A, Poldee S, Sriratanasathavorn C. Plasma lipid peroxidation and antioxidiant nutrients in type 2 diabetic patients. J Med Assoc Thai 2006;89(Suppl. 5):S147–S155
48. Baldeiras I, Santana I, Proença MT, et al. Peripheral oxidative damage in mild cognitive impairment and mild Alzheimer's disease. J Alzheimers Dis 2008;15:117–128
49. Zemlan FP, Thienhaus OJ, Bosmann HB. Superoxide dismutase activity in Alzheimer's disease: possible mechanism for paired helical filament formation. Brain Res 1989;476:160–162
50. Li ZG, Zhang W, Sima AA. Alzheimer-like changes in rat models of spontaneous diabetes. Diabetes 2007;56:1817–1824